

Effects of Elevated Temperatures on Ballistic Resistance of Ultra High Molecular Weight Polyethylene

Thore Heurich, Arash Ramezani and Hendrik Rothe

Chair of Measurement and Information Technology

University of the Federal Armed Forces

Hamburg, Germany

Email: thore.heurich@hsu-hh.de, ramezani@hsu-hh.de, rothe@hsu-hh.de

Abstract—In the security sector, the partly insufficient safety of people and equipment due to failure of industrial components are ongoing problems that cause great concern. The temperature resistance of cross-ply oriented ultra high molecular weight polyethylene (UHMWPE) is an important thermomechanical property for using this material under different environmental conditions. Therefore, it is essential for the safety of people inside the armored vehicle to know the ballistic resistance at elevated temperatures.

Keywords—solver ballistic resistance; elevated temperatures; fiber-reinforced plastics; armor systems.

I. INTRODUCTION

Nowadays, fiber reinforced composites are used in numerous technical areas. In contrast to other materials like steel or aluminum, they have the advantage of the same mechanical strength at less weight.

This work will focus on composite armor structures consisting of several layers of ultra-high molecular weight polyethylene (UHMWPE), a promising ballistic armor material due to its high specific strength and stiffness. The goal is to evaluate the ballistic resistance of UHMWPE composite at elevated temperatures.

While soft armor packages used in body armor have to withstand temperatures up to 70 °C, there are hard armor panels which have to withstand even higher temperatures. Hard armor panels are used in security vehicles where the temperature can reach up to 110 °C. In this study, the temperature dependent ballistic resistance of hard armor panels made of Dyneema[®] HB26 is analyzed. Therefore, the theoretical background of the thermomechanics of fiber reinforced composite is presented. Furthermore, practical tests were performed to show the influence of temperature on the ballistic resistance. Panels with different thicknesses were shot with three types of ammunition at room temperature (20 °C) and at elevated temperatures (up to 110 °C) to compare their ballistic performance at different environmental conditions.

The rest of the paper is structured as follows. Section II presents the state of the art. Section III introduces thermomechanical principles relevant to this work. Section IV presents and discusses the ballistic trials. We conclude in Section V.

II. STATE-OF-THE-ART

Fundamental studies about the laminate theory were performed in [1]. In this work, Mittelstedt presented calculation methods to describe the mechanical characteristics of laminates. In thermoplastics, the degree of crystallization essentially determines the mechanical properties of the material, which is described in [2, 3].

Further literature describes construction rules, where the influence of the temperature on the material is explained. For example, the coefficients of thermal expansion for different materials are given in [4]. The deformation caused by the change of temperature results in thermal stress, presented in [5].

In order to investigate the thermal effects on UHMWPE, it is essential to know the temperature in the application area of the material. A lot of researches exist in this field, so only the most important are mentioned. First, there are practice tests about temperature variations in automobiles in various weather conditions [6, 7]. Additional simulations in [8, 9] show the highest temperatures under extreme environmental conditions, which are 110 °C at the vehicle roof and up to 165 °C near the exhaust system. UHMWPE cannot be used under these conditions, because it has a too low melting temperature, at around 135-138 °C [10].

Cunniff made important researches to define the ballistic resistance of different materials by adding the Cunniff-parameter in [11]. This parameter correlates well with the limit velocity V_{50} , where 50 % of the bullets perforate the target. Moreover, the dependence of V_{50} and the areal density (AD) of Dyneema[®] composites is analyzed in [12].

Similar investigations, such as those in this study, are made by Meulmann et al. in [13, 14]. First, they analyze the aging of Dyneema[®] HB26 in thermal long-term tests, then they performed ballistic tests on HB26 at 90 °C with 7.62×39 mm MSC-projectiles.

III. THERMOMECHANICAL PRINCIPLES

The constitutive equations describe the connectivity between stress σ and strain ε of an elastic deformed body and are summarized in the linear elastic material law. To describe the state of an elastic body under load, the one-dimensional Hooke's Law is needed:

$$\sigma = E\varepsilon \quad (1)$$

where E describes the tensile modulus.

The three-dimensional form depends on the different directions of deformations ε_{ij} and γ_{ij} , of the values S_{ij} of the symmetric compliance matrix and of the stress σ_{ij} and τ_{ij} . Therefore, the first index defines the direction of the surface normal and the second index the direction of the deformation or stress.

$$\begin{bmatrix} \varepsilon_{11} \\ \varepsilon_{22} \\ \varepsilon_{33} \\ \gamma_{23} \\ \gamma_{13} \\ \gamma_{12} \end{bmatrix} = \begin{bmatrix} S_{11} & S_{12} & S_{13} & S_{14} & S_{15} & S_{16} \\ S_{12} & S_{22} & S_{23} & S_{24} & S_{25} & S_{26} \\ S_{13} & S_{23} & S_{33} & S_{34} & S_{35} & S_{36} \\ S_{14} & S_{24} & S_{34} & S_{44} & S_{45} & S_{46} \\ S_{15} & S_{25} & S_{35} & S_{45} & S_{55} & S_{56} \\ S_{16} & S_{26} & S_{36} & S_{46} & S_{56} & S_{66} \end{bmatrix} \begin{bmatrix} \sigma_{11} \\ \sigma_{22} \\ \sigma_{33} \\ \tau_{23} \\ \tau_{13} \\ \tau_{12} \end{bmatrix} \quad (2)$$

The compliance matrix can be calculated out of the tensile moduli E_{ij} , shear moduli G_{ij} and poisson's ratios ν_{ij} . Also, a laminate is an orthotropic material with symmetrical planes, so there are some values in the compliance matrix, which become zero. Besides the deformation caused by mechanical stress, there is a deformation caused by the change of temperature ΔT .

$$\begin{bmatrix} \varepsilon_{11} \\ \varepsilon_{22} \\ \varepsilon_{33} \\ \gamma_{23} \\ \gamma_{13} \\ \gamma_{12} \end{bmatrix} = \begin{bmatrix} \frac{1}{E_{11}} & -\frac{\nu_{21}}{E_{22}} & -\frac{\nu_{31}}{E_{33}} & 0 & 0 & 0 \\ -\frac{\nu_{12}}{E_{11}} & \frac{1}{E_{22}} & -\frac{\nu_{32}}{E_{33}} & 0 & 0 & 0 \\ -\frac{\nu_{13}}{E_{11}} & -\frac{\nu_{23}}{E_{22}} & \frac{1}{E_{33}} & 0 & 0 & 0 \\ 0 & 0 & 0 & \frac{1}{G_{23}} & 0 & 0 \\ 0 & 0 & 0 & 0 & \frac{1}{G_{13}} & 0 \\ 0 & 0 & 0 & 0 & 0 & \frac{1}{G_{12}} \end{bmatrix} \begin{bmatrix} \sigma_{11} \\ \sigma_{22} \\ \sigma_{33} \\ \tau_{23} \\ \tau_{13} \\ \tau_{12} \end{bmatrix} + \Delta T \begin{bmatrix} \alpha_{11}^T \\ \alpha_{22}^T \\ \alpha_{33}^T \\ 0 \\ 0 \\ 0 \end{bmatrix} \quad (3)$$

In an orthotropic material, only the first three coefficients of thermal expansion α_{ij}^T are nonzero, so they cause only a strain state. Because of different coefficients of thermal expansion and orientation of fiber and matrix in the laminate, thermal expansion can result in thermal stress.

Moreover, plastics show three different temperature-dependent states, plotted in Figure 1. First, there is the energy-elastic area, where the material shows glassy and brittle

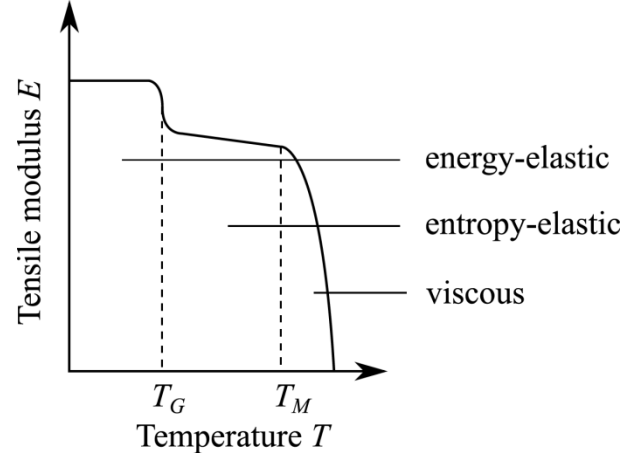


Figure 1. Energy-elastic, entropy-elastic and viscous area of thermoplastics shown at the tensile modulus E as a function of the temperature T .

behavior. In the entropy-elastic area, the material shows tough behavior and the mechanical strength values decrease slowly at higher temperatures. At the melting temperature T_M , the material loses its stiffness so the mechanical strength values fall to zero, which is why this area is called the viscous area.

The temperature also influences the fail-tension σ_f and fail-elongation ε_f of a thermoplastic, shown in Figure 2. Higher temperatures cause a decrease in fail tension and increase in fail-elongation, so the material can be more deformed until it cracks.

To make a connection between the temperature-dependent mechanical values and the ballistic resistance of fiber-reinforced plastics, Cunniff introduced the parameter

$$U = \frac{1}{2} \frac{\sigma_f \varepsilon_f}{\rho} \sqrt{\frac{E}{\rho}} \quad (4)$$

which depends on the material parameters of the fibers, like the density ρ . The Cunniff-parameter $U^{1/3}$ correlates well with the limit velocity V_{50} , where the bullet perforates the target by a probability of 50 %.

IV. BALLISTIC TRIALS

Ballistics is an essential component for the evaluation of our results. Here, terminal ballistics is the most important sub-field. It describes the interaction of a projectile with its target. Terminal ballistics is relevant for both small and large caliber projectiles. The task is to analyze and evaluate the impact and its various modes of action. This will provide information on the effect of the projectile and the extinction risk.

A. Experimental set-up

To analyze the decrease of the ballistic resistance at elevated temperatures, the test results at room temperature

(20 °C) are used as reference values for the following tests. Therefore, the experimental set-up shown in Figure 3 is used. Ballistic tests are recorded with high-speed videos and analyzed afterwards. Testing was undertaken at an indoor

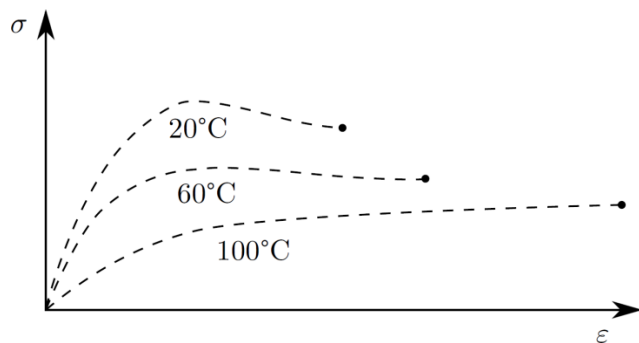


Figure 2. Qualitative effects of the temperature on the stress-strain-diagram of thermoplastics with decreasing fail-stress σ_f and increasing fail-strain ϵ_f at higher temperatures.

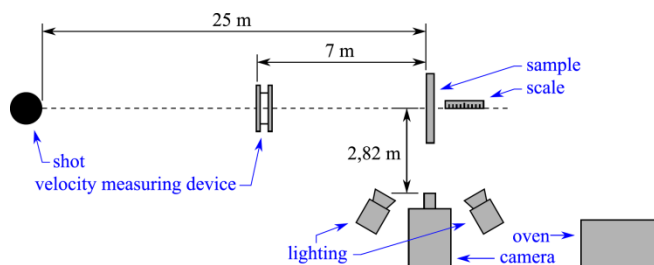


Figure 3. Experimental set-up.

testing facility. The target stand provides support behind the target on all four sides. The camera system is a PHANTOM v1611 that enables fast image rates up to 646,000 frames per second (fps) at full resolution of 1280 x 800 pixels. Because of the short time lapse of about 2ms and the high fps, three powerful plasma spotlights Hive Wasp Plasma Par were used for lighting with nearly 178,000Lx.

The oven Hamilton Beach 22 Quart Roaster Oven has to be placed near the sample to ensure a fast attachment of the panels. Before the test execution, analyses about the cooling rate of the panels with different thicknesses have been performed. For this purpose, the surface temperature was measured with an infrared thermometer Bosch GIS 100C Professional and the core temperature was measured with a temperature sensor Greisinger GMH 3710. These tests have shown that the surface temperature is cooling too fast from the temperature of the oven $T_0 = 125$ °C to the boundary-temperature $T_B = 110$ °C. Nevertheless, it can be ensured that the core temperature of plates made by 40 plies of HB26 is still over 110 °C within the first 2 minutes after removing them from the oven.

B. Test execution

As described above, this experiment is based on the results of ballistic tests at room temperature, so three

different projectiles were fired at the HB26 plates which stopped the projectile in these reference tests. So, the projectiles 9×19 mm Luger FMJ, 7.62×39 mm Kalaschnikow MSC and 7.62×51 mm NATO FMJ were fired at plates with 20, 40 or 60 plies of HB26 with a core temperature of at least 110 °C. Additional measurements have shown that 20 plies have a thickness of 5.5 mm, 40 plies a thickness of 11.0 mm and 60 plies a thickness of 16.2 mm. It is important that the impact velocity is nearly the same at room temperature and elevated temperature to ensure comparability between both experiments.

The next important fact is that the plates have to heat up in the oven for at least 2 hours. In this way, it is guaranteed that the core temperature reaches the boundary-temperature of 110 °C during the impact.

C. Test results

After the ballistic trials at elevated temperatures, the results have to be prepared carefully to compare them with the results of the measurements at room temperature. For this purpose, the following parameters out of the video-analyses and static measurements are used:

1) *Impact velocity*: The impact velocity v_i will be measured to ensure the comparability between the tests with the same ammunition. Besides the environmental influences, the variations in the amount of propellant in the ammunition pose a problem.

2) *Perforation*: This is the easiest and most important way to evaluate these ballistic tests. Therefore, only the fact of a successful or unsuccessful perforation is used.

3) *Remaining velocity or thickness*: Based on the previous evaluation of a perforation, there are two more parameters for a comparison. For one thing the remaining velocity v_r after a successful perforation measured in the video, for another thing the remaining thickness of the plate x_r after a unsuccessful perforation measured at the undeformed corner of the plates because of the compression of the material at the impact zone.

4) *Buckling diameter and depth*: The decisive factor for a real usage is the space taken by the dynamic deformation during the impact, because this space is mostly limited in constructions. Hence, the buckling diameter a and buckling depth b were measured in the video when the buckling is at the maximum, seen in Figure 4.

First, the 9×19 mm Luger FMJ-projectile is fired at plates made of 20 plies of Dyneema® HB26. In Figure 5, the maxima of buckling at room temperature (left) and at elevated temperature (right) are shown to compare the qualitative deformation. The deformation characteristics of both tests show no significant difference. The measured parameters for comparison are given in Table I.

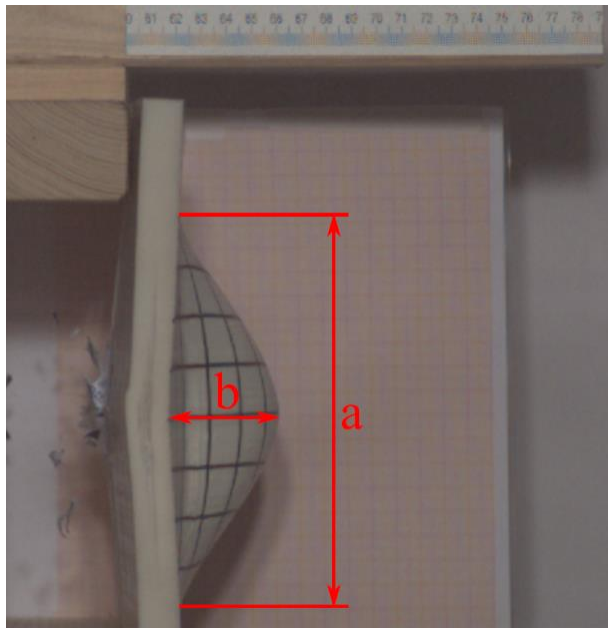


Figure 4. Measuring the buckling diameter a and the buckling depth b at the maximum of the dynamic deformation.

TABLE I. COMPARISON BETWEEN THE MEASURED RESULTS OF 20 PLIES DYNEEMA® HB26 IMPACTS BY A 9X19 mm JMF BULLETS 20 °C AND 110 °C.

	Room temp.	Elevated temp.
Impact velocity	348 m/s	316 m/s
Perforation	no	no
Remaining velocity	0 m/s	0 m/s
Remaining thickness	4.5 mm	4.9 mm
Buckling diameter	224 mm	202 mm
Buckling depth	27 mm	34 mm

The test at elevated temperature has shown a 9.2 % lesser impact velocity than the test at room temperature, but a larger buckling depth. The reason for these results is the changing mechanical values, as explained above. In connection therewith the thermoplastic becomes tougher and the fail-elongation ϵ_f increases at higher temperatures. Indeed, the deformation is a little bit larger at elevated temperature, but the ballistic resistance remains nearly constant for low-energy projectiles like 9×19 mm FMJ.

The second analyzed projectile is 7.62×39 mm Kalaschnikow FMJ. Here, the ballistic tests at both temperatures have a deviation of their impact velocity of 2.9 %. While the bullet gets stopped easily by a 60 plies HB26 plate at room temperature with a remaining thickness of nearly a third of the initial thickness, the ballistic resistance of HB26 decreases critically at elevated temperature. As seen in Figure 6, the bullet perforates a headed up 60 plies HB26 plate and loses only 19.6 % of the velocity trough energy release. Because the buckling has nearly the same



Figure 5. Effect of 20 plies Dyneema® HB26 impacts by a 9×19 mm FMJ bullets at 20 °C (left) and 110 °C (right), 507 μ s and 774 μ s after the initial impact.

TABLE II. COMPARISON BETWEEN THE MEASURED RESULTS OF 60 PLIES DYNEEMA® HB26 IMPACTS BY A 7.62X39 mm JMF BULLETS 20 °C AND 110 °C.

	Room temp.	Elevated temp.
Impact velocity	674 m/s	708 m/s
Perforation	no	yes
Remaining velocity	0 m/s	569 m/s
Remaining thickness	10.9 mm	-
Buckling diameter	224 mm	-
Buckling depth	27 mm	-

size in both tests, it is obvious that the decrease of the fail-tension σ_f is the dominating problem here.

Finally, the standardized NATO projectile 7.62×51 mm FMJ will be fired at 60 plies HB26 plates. Both pictures out of the video analysis are shown in Figure 7 and the measured parameters are given in Table III. Although the impact velocity of both ballistic tests are exactly the same (measuring errors are neglected), there is an obvious difference in the results. The result of the bullet fired at the HB26 plate at room temperature causes initial approaches of delamination at the margins, but has not enough energy for a perforation. At elevated temperature, the bullet does not break up all plies, but causes a fully delamination of the plate. This result gets classified as a successful perforation, because the plies at the far end get detached from the rest and will be accelerated in the firing direction. The reason for the delamination is the failing matrix, which cannot transfer the forces between the fibers because of the decreased strength.



Figure 6. Effect of 60 plies Dyneema®HB26 impacts by a 7.62×39 mm FMJ bullets at 20 °C (left) and 110°C (right), 265 μs and 53 μs after the initial impact.

TABLE III. COMPARISON BETWEEN THE MEASURED RESULTS OF 60 PLIES DYNEEMA® HB26 IMPACTS BY A 7.62X19 mm JMF BULLETS 20 °C AND 110 °C.

	Room temp.	Elevated temp.
Impact velocity	819 m/s	819 m/s
Perforation	no	yes
Remaining velocity	0 m/s	-
Remaining thickness	6.4 mm	4.2
Buckling diameter	144 mm	-
Buckling depth	42 mm	-



Figure 7. Effect of 60 plies Dyneema®HB26 impacts by a 7.62×51 mm FMJ bullets at 20 °C (left) and 110°C (right), 409 μs and 2050 μs after the initial impact.

V. CONCLUSIONS

This paper examines the effects of elevated temperatures on ballistic resistance of ultra high molecular weight polyethylene. Therefore, ballistic trials with different projectiles were fired at plates made of Dyneema® HB26 plies.

At the beginning, the thermomechanical principles of thermoplastic composites were presented. Starting from the one-dimensional Hooke's Law, the three-dimensional linear elastic material law was established. After this, the deformations caused by the change of temperature were introduced and added to the linear elastic material law. These deformations can lead to thermal stress in the material.

Afterwards, the temperature-dependend states of plastics were explained on mechanical strength values. These include the energy-elastic area, the entropy-elastic area and the viscous area. In connection with this, the effect of the temperature on the stress-strain-diagram of plastic is shown.

Completing the thermomechanical principles, the Cunniff-parameter was presented to connect the mechanical parameters with the ballistic resistance in one equation.

Finally, ballistic trials were performed, where plates made of 20 or 60 Dyneema® HB26 plies were fired first at 20 °C and then at 110 °C. Therefore, the projectiles 9×19 mm Luger FMJ, 7.62×39 mm Kalschnikow FMJ and 7.62×51 mm NATO FMJ were used. High-speed videos were used to analyse the characteristics of the deformation during the impact. Subsequently, the results were qualitatively and quantitatively compared. The results have shown that the ballistic resistance has a low to high lack at elevated temperatures, depending of the type of projectile.

REFERENCES

- [1] C. Mittelstedt, W. Becker. 2012. "Strukturmechanik ebener Laminare."
- [2] H. Dominghaus, P. Elsner, P. Eyerer, T. Hirth. 2012. "Kunststoffe: Eigenschaften und Anwendungen," Berlin, Springer Verlag.
- [3] A. Franbourg, F. Rietsch. 1990. "Influence of the melt temperature on the thermoplastics crystallization process," in *Polymer bulletin*, pp. 445-450.
- [4] H. Schürmann, 2005. "Konstruieren mit Faser-Kunststoff-Verbunden," Berlin, Springer Verlag.
- [5] W. Schneider, 1977. "Thermische Ausdehnungskoeffizienten und Wärmespannungen faserverstärkter Kunststoffe," *Kohlenstoff- und aramidfaserverstärkten Kunststoffen*. Düsseldorf. VDI Verlag.
- [6] W. Marty, T. Sigrist, D. Wyler, 2001. "Temperature variations in automobiles in various weather conditions: An experimental contribution to the determination of time of death," in *The American journal of forensic medicine and pathology* 22, pp. 215-219.
- [7] Volkswagen-AG, 2004 "Vehicle parts - Testing of Resistance to Environmental Cycle test," PV 1200 Klass.-Nr. 50321.

- [8] S. Schlegl, 2016 “Schutzkonzepte für zivile Sicherheitsfahrzeuge,” presented at Carl-Cranz-Gesellschaft e.V. in Lichtenau, Germany.
- [9] E. T. Hasegawa, 2008. “Simulation der thermischen Verhältnisse in Motorräumen mit CFD,” in *ATZ-Automobiltechnische Zeitschrift* 110, pp. 330-335.
- [10] J. P. Attwood, S. N. Khaderi, K. Karthikeyan, N. A. Fleck, M. R. O'Masta, H. Wadley, V. S. Deshpande. 2014. “The out-of-plane compressive response of Dyneema composites,” in *Journal of the Mechanics and Physics of Solids* 70, pp. 200-226
- [11] P. M. Cunniff, 1999. “Dimensionless parameters for optimization of textile-based body armor systems,” in *Proceedings of the 18th International and Symposium on Ballistics*, pp. 1303-1310.
- [12] M. J. N. Jacobs, J. L. J. Van Dingenen. 2001. “Ballistic protection mechanisms in personal armour,” in *Journal of Materials Science* 36, pp. 3137-3142.
- [13] J. H. Meulman, H. van der Werf, S. Chabba, A. Vunderink. 2010. “Ballistic performance of Dyneema® at elevated temperatures, extreme for body armor,” in *Proceedings Personal Armor System Symposium*. Quebec.
- [14] J. H. Meulman, 2012. “Ballistic performance of Dyneema® at elevated temperatures, extreme for body armor - part 2.”